Finding the "Correct" Shell Model

Let us consider one nucleon of mass m moving in a spherically symmetric potential, $V(r)$. The Schrödinger equation for this problem in three dimensions is the same as Equation 7-9. Since we are assuming $V(r)$ to be independent of θ and ϕ, the angular part of the equation can be separated and solved, as discussed in Chapter 7. The result is that the square of the angular momentum is restricted to the values $\ell(\ell + 1)\hbar^2$ and the z component to the values $m_\ell\hbar$. The radial equation is then Equation 7-24 with $V(r)$ replacing the Coulomb potential:

$$-\frac{\hbar^2}{2mr^2}\frac{d}{dr}\left(r^2\frac{dR}{dr}\right) + \left[\frac{\ell(\ell+1)\hbar^2}{2mr^2} + V(r)\right]R = ER \qquad \textbf{11-56}$$

The solution of this equation, of course, depends on the form of the potential energy $V(r)$. Although $V(r)$ is not known, we certainly expect it to be quite different from the $1/r$ potential used in Chapter 7 for atoms. Because the nuclear force is so strong and is negligible beyond a few fermis of the nuclear surface, it does not matter too much what the exact form of $V(r)$ is. Various guesses have been made. The simplest is the finite square well (Figure 11-36*b*),

$$V(r) = -V_0 \qquad \text{for } r < r_N$$
$$V(r) = 0 \qquad \text{for } r > r_N$$

where r_N is the nuclear radius. This corresponds to an infinite attractive force at the nuclear surface and does not produce the correct magic numbers. Figure 11-37*a* shows the energy levels obtained for an infinite square well, and Figure 11-37*b* shows the levels for a finite well with rounded corners such as that of Figure 11-36*a*. This latter potential has the mathematical form

$$V(r) = \frac{-V_0}{(1 - e^{(r-R_0)/t})} \qquad \textbf{11-57}$$

where the radius R_0 and the skin thickness t are defined in Figure 11-5*b*. The levels are labeled with the number n and the spectroscopic notation s for $\ell = 0$, p for $\ell = 1$, etc. The number n is *not* the principal quantum number but simply an index that counts the levels with a particular ℓ value. For example, $1p$ is the lowest energy state with $\ell = 1$, $2p$ is the next lowest $\ell = 1$ state, and so on. The first number after the spectroscopic label in Figure 11-37*b* is the number of identical particles that can exist in that level. This number is $2(2\ell + 1)$; that is, $(2\ell + 1)$ different m_ℓ states times 2 for the two possible orientations of the spin. The second number is the total number of

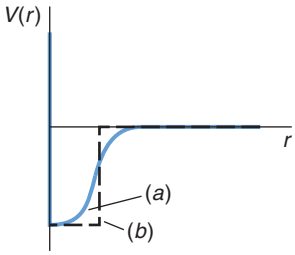

FIGURE 11-36 (*a*) Nuclear potential well with rounded corners. (*b*) Finite-square-well approximation.

particles up to and including that level. From this calculation we should expect the magic numbers to be 2, 8, 20, 40, 70, 92, and 138 since there are relatively large energy differences after these numbers. Although the first three numbers, 2, 8, and 20, do agree with the observed stability of ^{4}He ($N = 2$ and $Z = 2$), ^{16}O ($Z = N = 8$), and ^{40}Ca ($Z = N = 20$), the rest of the numbers are not the magic numbers observed. For example, there is no evidence from this figure for the magic number 50. Calculations using various other potential wells give about the same ordering and spacing of the energy levels.

Mayer and Jensen resolved this problem by proposing that the spin dependence of the nuclear force results in a very strong spin-orbit interaction, coupling the spin of each nucleon to its own orbital angular momentum. Thus, the nuclear spin-orbit effect depends on *j-j* coupling[20] rather than the *L-S* coupling that characterizes the electron spin-orbit interaction (see Section 7-5). This strong spin-orbit interaction results in a decrease in the energy if the spin and the orbital angular momentum of the nucleon are parallel and an increase if they are antiparallel. We have seen that in the atomic spin-orbit interaction, the energy of the atom depends on whether j is $\ell + 1/2$ or $\ell - 1/2$; however, this fine-structure splitting of the atomic energy levels is very small compared with the energy difference between the shells or subshells and can be neglected in the first approximation to atomic energies. The situation is different for nuclei. The strength of the interaction results in a large splitting of the energy for a given ℓ if ℓ is large. (The shell model does not provide a prediction of the required interaction strength. The strength is an adjustable parameter whose value is chosen to yield the observed energy structure of the nucleus.) Figure 11-38 shows the energy levels with the strong spin-orbit interaction proposed by Mayer and Jensen. As noted earlier, the levels with the spin and orbital angular momentum parallel have a lower energy than those with the spin and orbital angular momentum antiparallel; that is, the higher j values have lower energies, unlike the situation for atoms. (The fact that the force of attraction between a nucleon and a nucleus is greater when spin and orbital angular momentum of the nucleon are parallel can also be shown from scattering experiments.) Note, too, that the splitting is large for large ℓ values. Indeed, the splitting of the $1g$ level is so great that the large energy difference that occurs between the $1g_{9/2}$ ($n = 1$, $\ell = 4$, $j = \ell + s = 9/2$) and the $1g_{7/2}$ ($n = 1$, $\ell = 4$, $j = \ell - s = 7/2$) levels is enough to place those two sublevels in different major shells. Since there are $(2j + 1)$ values of m_j, there can be 10 neutrons or protons in the $1g_{9/2}$ level, making a total of 50 up through this level. The next large energy difference occurs because of the splitting of the $1h$ level, and this accounts for the magic number 82. Being distinct particles, the protons and neutrons occupy different sets of energy states. Figure 11-38 illustrates the energy spacing for protons, which, due to the electrostatic force, is slightly different than that for neutrons.

From qualitative considerations alone it is not possible to decide the exact order of the energy levels, for example, whether the $2s_{1/2}$ level is higher or lower than the $1d_{3/2}$ level. Questions of this nature can usually be answered from empirical evidence. As an example of the predictions of the shell model, we will consider a nuclide with one neutron or one proton outside a closed shell. These are the simplest nuclides (except for those with closed shells of both neutrons and protons) and are somewhat analogous to the alkali atoms with one outer electron. Many of the energy levels of these nuclides can be understood in terms of the excitation of the one odd nucleon. Table 11-5 lists several nuclei with one nucleon added to or removed from a closed

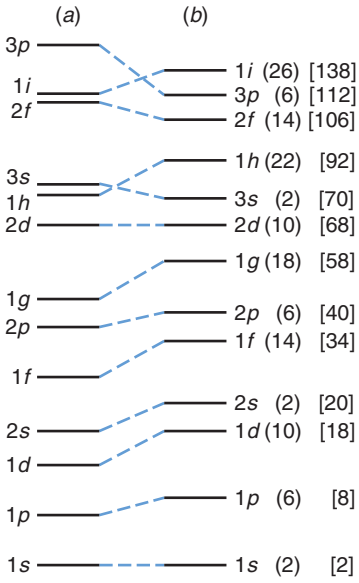

FIGURE 11-37 Energy levels for a single particle in (*a*) an infinite square well and (*b*) a finite square well with rounded corners such as shown in Figure 11-36*a*. The maximum number of particles in each level is given in parentheses, followed by the total number through that level in brackets.

shell or subshell along with the predicted state of this nucleon and the measured spin and magnetic moment of the nucleus. In all these cases but one, the spin prediction is correct. This simple shell model is also reasonably successful in predicting the magnetic moments for these nuclei. For example, the magnetic moment of ^{17}O is observed to be -1.89, which is quite close to that of a single neutron. This is predicted by the shell model for this nucleus since the other eight neutrons and the eight protons each form a closed shell. Similarly, the magnetic moment of ^{11}B is $+2.69$, very close to that of the odd proton, and that of ^{41}Ca is -1.60, close to that of the odd neutron. In general, however, the measured values of the magnetic moments for odd A nuclei do not agree with the simple model that attributes them solely to the odd nucleon. For a more complete discussion of the success of this shell model, the reader may enjoy perusing Mayer and Jensen's excellent book (1955).

The most serious deficiency of the simple shell model is in the region of the rare earth nuclei. The quadrupole moments predicted from the orbital motion of the individual protons are much smaller than those observed. Many of the excited states of these nuclei can be more simply understood as being due to the rotation or vibration of the nucleus as a whole if it is considered to be a deformed liquid drop. From the shell-model point of view, the rare earth nuclei lie about midway between the neutron magic numbers of 82 and 126. This is just the region for which shell-model calculations are the most difficult since there are many particles outside a closed shell. There are several extensions of the shell model that have been fairly successful in allowing us to understand these nonspherical nuclei. In one of these, called the *collective model*, the closed-shell core nucleons are treated as a liquid drop deformed by the interaction with the outer nucleons that orbit about the core and drag it along with them. In another model, called the *unified model*, the Schrödinger equation is solved

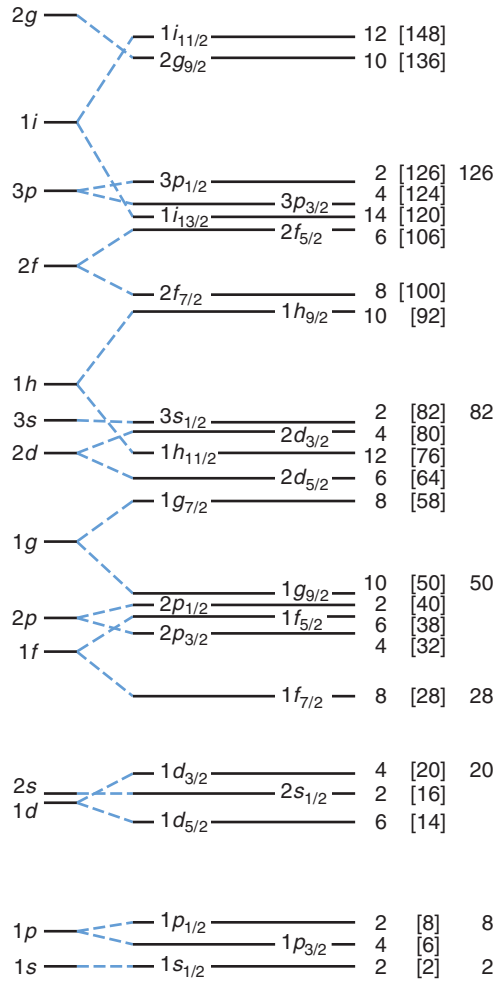

FIGURE 11-38 Energy levels for a single particle in a nuclear well, including spin-orbit splitting. The maximum number of particles in each level is given at the right, followed by the total number through that level in brackets. The total numbers just before the large energy gaps are the magic numbers. The spacing shown here is for protons; the spacing for neutrons is slightly different (lower).

Table 11-5 Angular momenta and magnetic moments of selected odd-*A* nuclei

Isotope	Number of odd particles	*Z* or *N*, a magic number	Predicted level	Measured spin	Measured magnetic moment (μ_N)
$^{11}_{5}B_6$	5	–	$p_{3/2}$	3/2	+2.689
$^{13}_{6}C_7$	7	–	$p_{1/2}$	1/2	+0.702
$^{15}_{7}N_8$	7	N	$p_{1/2}$	1/2	−0.283
$^{17}_{8}O_9$	9	Z	$d_{5/2}$	5/2	−1.894
$^{17}_{9}F_8$	9	N	$d_{5/2}$	5/2	+4.722
$^{27}_{13}Al_{14}$	13	–	$d_{5/2}$	5/2	+3.641
$^{39}_{19}K_{20}$	19	N	$d_{3/2}$	3/2	+0.09
$^{41}_{20}Ca_{21}$	21	Z	$f_{7/2}$	7/2	−1.595
$^{41}_{21}Sc_{20}$	21	N	$f_{7/2}$	7/2	–
$^{57}_{28}Ni_{29}$	29	Z	$p_{3/2}$	3/2	–
$^{91}_{40}Zr_{51}$	51	–	$g_{7/2}$	5/2	−1.303
$^{115}_{49}In_{66}$	49	–	$g_{9/2}$	9/2	–
$^{205}_{81}Tl_{124}$	81	–	$s_{1/2}$	1/2	+1.628
$^{209}_{83}Bi_{126}$	83	N	$h_{9/2}$	9/2	+4.080

for individual particles in a nonspherically symmetric potential corresponding to an ellipsoidal nucleus. Much of the work with these models was done by J. Rainwater, A. Bohr (son of Niels Bohr), and B. Mottleson, who shared the 1975 Nobel Prize in Physics for this work.